World Academy of Science, Engineering and Technology
International Journal of Medical and Health Sciences
Vol:2, No:1, 2008

Neural Network based Texture Analysis of Liver Tumor from Computed Tomography Images

K.Mala, V.Sadasivam, and S.Alagappan

***Abstract*—**Advances in clinical medical imaging have brought about the routine production of vast numbers of medical images that need to be analyzed. As a result an enormous amount of computer vision research effort has been targeted at achieving automated medical image analysis. Computed Tomography (CT) is highly accurate for diagnosing liver tumors. This study aimed to evaluate the potential role of the wavelet and the neural network in the differential diagnosis of liver tumors in CT images. The tumors considered in this study are hepatocellular carcinoma, cholangio carcinoma, hemangeoma and hepatoadenoma. Each suspicious tumor region was automatically extracted from the CT abdominal images and the textural information obtained was used to train the Probabilistic Neural Network (PNN) to classify the tumors. Results obtained were evaluated with the help of radiologists. The system differentiates the tumor with relatively high accuracy and is therefore clinically useful.

***Keywords*—**Fuzzy C Means Clustering, Texture analysis, Probabilistic Neural Network, LVQ Neural Network

I. Introduction

THE most common medical imaging studies for early detection and diagnosis of liver tumors include UltraSonography (US), Computed Tomography (CT), Magnetic Resonance (MR) Imaging and Angiography [1]. Although Ultrasonography is non invasive and does not emit radiation, it is operator dependent. Furthermore, the images are non specific for diagnosing benign, malignant tumors and their subtypes based on echogenecity. MR Imaging with its endogenous high tissue contrast and multiplanar capability can accurately detect and differentiate liver tumors. However, the examination is very expensive and therefore is not as popular as CT. Angiography is an invasive procedure with potential complications.

Diagnostic accuracy can be improved by providing additional information that cannot be obtained by simple visual interpretation. As a result, Computer Aided Diagnosis (CAD) has become one of the major research subjects in medical imaging and diagnostic radiology [2].

The general CAD system for liver diseases can be divided into three parts. The first part is the extraction of the liver image from CT abdominal image. The second part is the suitable feature extraction from the liver image to characterize the different liver tissues. The third part is the classification of the liver diseases.

Chung-Ming Wu, et al. [3] proposed a texture feature called Multiresolution Fractal (MF) feature to distinguish normal, hepatoma and cirrhosis liver using ultrasonic liver images with an accuracy of 90%.

Yasser M. Kadah, et al. [4] extracted first order gray level parameters like mean and first percentile and second order gray level parameters like Contrast, Angular Second Moment, Entropy and Correlation, and trained the Functional Link Neural Network for automatic diagnosis of diffused liver diseases like fatty and cirrhosis using ultrasonic images and showed that very good diagnostic rates can be obtained using unconventional classifiers trained on actual patient data.

Aleksandra Mojsilovic, et al. [5] investigated the application and advantages of the non separable wavelet transform features for diffused liver tissue characterization using B-Scan liver images and compared the approach with other texture measures like SGLDM (Spatial Gray Level Dependence Matrices), Fractal texture measures and Fourier measures. The classification accuracy was 87% for the SGLDM, 82% for Fourier measures and 69% for Fractal texture measures and 90% for wavelet approach.

E-Liang Chen, et al. [6] used Modified Probabilistic Neural Network (MPNN) on CT abdominal images in conjuction with feature descriptors generated by fractal feature information and the gray level co occurrence matrix and classified liver tumors into hepatoma and hemangeoma with an accuracy of 83%.

Pavlopoulos, et al. [7] proposed a CAD system based on texture features estimated from Gray Level Difference Statistics (GLDS), SGLDM, Fractal Dimension (FD) and a novel fuzzy neural network classifier to classify a liver ultrasound images into normal, fatty and cirrhosis with accuracy in the order of 82.7%.

Jae-Sung Hong, et al. [8] proposed a CAD system based on Fuzzy C Means Clustering for liver tumor extraction with an accuracy of 91% using features like area, circularity and minimum distance from liver boundary to tumor and Bayes classifier for classifying normal and abnormal slice.

Manuscript received on October 26, 2006.

K.Mala is currently pursuing Ph.D. under the guidance of Dr.V.Sadasivam in Manonmaniam Sundaranar University, Tirunelveli, Tamilnadu, India. Also working in Mepco Schlenk Engineering college, Sivakasi, Tamilnadu, India. Email : kmala@mepcoeng.ac.in; mala_k21@yahoo.co.in

Dr.V.Sadasivam is currently working as a Professor and Head in Computer Science and Engineering Department in Manonmaniam Sundaranar University, Tirunelveli, Tamilnadu, India. Email: vs_raghav@sancharnet.in

Dr.S.Alagappan, M.D. is currently working as a Chief Radiologist in Devaki MRI & CT Scans, Madurai, Email: alagappan_sl@rediffmail.com

The CAD system proposed by Gletsos Miltiades, et al. [9] consists of two basic modules: the feature extraction and the classifier modules. In their work, region of interest (liver tumor) were identified manually from the CT liver images and then fed to the feature extraction module. The total performance of the system was 97% for validation set and 100% for testing set.

Haralick transform and Hopfield Neural Network were used to segment 90% of the liver pixels correctly from the CT abdominal image by John. E. Koss, et al. [10]. However, texture based segmentation results in coarse and blockwise contour leading to poor boundary accuracy.

Chien-Cheng Lee, et al. [11] identified liver region by using the fuzzy descriptors and fuzzy rules constructed using the features like location, distance, intensity, area, compactness and elongated-ness from CT abdominal images.

Wen-Li Lee et al. [12] proposed a feature selection algorithm based on fractal geometry and M-band wavelet transform for the classification of normal, cirrhosis and hepatoma ultrasonic liver images. A hierarchial classifier which is based on the proposed feature extraction algorithm is at least 96.7% accurate in distinguishing between normal and abnormal liver images and is at least 93.6% accurate in distinguishing between cirrhosis and hepatoma liver images.

Yu-Len Huang, et al. [13] used autocorrelation features and Multilayer Perception (MLP) Neural Network for predicting malignancies in the order of 80.5% from Non enhanced CT images. This reduced the need for iodinated contrast agent injection in CT examinations.

The literature survey shows that the tumor region is classified without identifying tumor region from liver region. Also, they don't classify the subcategories of benign and malignant tumor. In this regard, this study focused on the design and the development of a CAD system for classifying the liver tumors using wavelet based texture analysis and neural network.

II. METHODOLOGY

In this work, the image of the liver is automatically extracted from CT abdominal images using the anatomic knowledge of the liver, adaptive threshold decision based on intensity information and morphological processing. Tumor region is extracted using Fuzzy C Means Clustering (FCM). Biorthogonal wavelet transform is applied on the extracted tumor region to get Horizontal, Vertical and Diagonal details of images. For these three images SGLDM is constructed and the second order statistical features or co occurrence features are extracted. The selected feature set is used to train the Probabilistic Neural Network (PNN) to classify the liver tumor. The system outline is given in Fig. 1.

A. Image Acquisition

The data used in this work were collected from Devaki MRI & CT Scans, Madurai. The areas of interest of the CT abdominal images were captured by SOMATOM Emotion Duo CT Scanner. Plain spiral CT scanning of liver was scanned from the right dome of diaphragm to just below the inferior border of the liver using 8mm slices at 8mm interval with 0mm interslice gap. 70 mAs technique was used with 110 KVP, field of Vision (foV) 280 and image matrix of 256 x 256. 100 to 120 cc of omnipaque 350 was injected intravenously at the rate of 3cc per second and post contrast spiral CT scanning was done with 8mm slices at 8mm interval with 0mm interslice gap with scan delay of 30 seconds and 20 second spiral scanning with a pitch of 1.

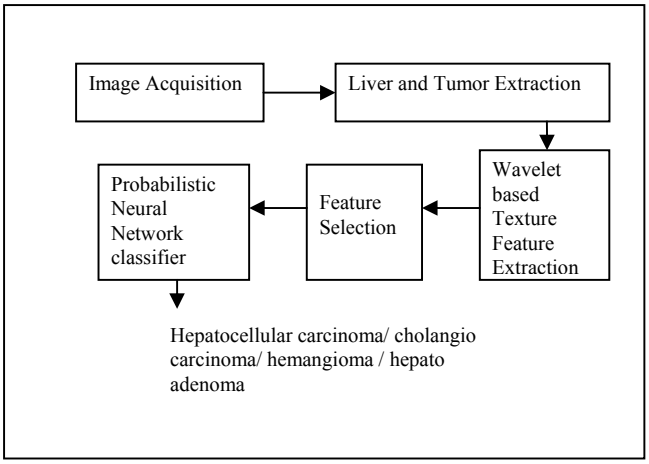

Fig. 1 System Outline

B. Liver and Tumor Extraction

Identifying liver from CT abdominal image has always been a challenging task. This is mainly due to the fact that there are other organs, with same intensity as liver, adjacent to the liver makes segmentation more difficult.

In this work liver and tumor regions are extracted by the following 3 steps. In the first step using anatomic knowledge of the liver and histogram analyzer, adaptive threshold is fixed to extract the liver pixels from the CT abdominal image which usually contains other organs including stomach, kidney, spleen, pancreas, etc. In the second step, morphological operations like closing and opening are used to preserve the structure of the liver and to remove the small fragments of other organs adjacent to the liver with the same intensity as that of liver. In the third step, tumor region is extracted using FCM Clustering technique, which can determine threshold regardless of a changing intensity. These steps are simple, reliable and extracting the region of interest correctly.

Normally, the liver is located on the upper left side of the image and takes up the largest area among the various organs included in the abdominal image. Even though, the liver region maintains a constant intensity throughout, a fixed threshold is not possible because the intensity differs according to the patient slice and the CT machine. Therefore, a system has to be developed to extract the liver automatically with adaptive threshold decision.

For the CT abdominal image, a window is fixed by removing the last 30 rows and 50 columns from the right since this area usually does not contain liver region. A histogram is drawn and analyzed for an area inside the window. The highest pitch excluding the background and bone values represent the middle intensity of the liver region. Certain margin is included within the intensity range of the liver region to accommodate any variance in the liver region pixels. Based on these processes, the proper intensity range corresponding to the liver region can be adaptively obtained for each slice. The pixels in the determined range of intensity are extracted. The output looks like scattered sand. It is converted to an object with real area using morphological closing and opening. Mathematical morphological operations tend to simplify image data preserving their essential shape characteristics and eliminating irrelevancies. Opening an image with a disk structuring element smoothes the contour, breaks narrow isthmuses, and eliminates small islands and sharp peaks or capes. Closing an image with a disk structuring element smoothes the contours, fuses narrow breaks and long thin gulfs, eliminates small holes, and fill gapes on the contours [14].

The liver is extracted along with the fragments of other organs located near to it and with the intensity same as that of liver. Based on certain conditions, the fragments of adjacent organs can be removed. The first condition is the location of the object. The liver is located in a constant area in the upper left side of the image. The second condition is the area. The area of the liver is large when it is compared with the fragments of other organs. After removing the fragments, the image obtained is complemented and multiplied with the original image to get the segmented liver in the CT abdominal image.

From the liver, tumor region is segmented using, FCM clustering technique. FCM minimizes the object function through the iterative optimization of the membership function based on the similarity between the data and the center of a cluster. FCM varies the threshold between clusters through an iterative process. As a result, the threshold is determined appropriately for every slice and the tumor region can be successfully extracted. $J_m(U,v)$ is the object function and u_{ik} is the membership function, are defined using the equations (1) and (2)

$$J_m(U,v) = \sum_{k=1}^{n}\sum_{i=1}^{c}(u_{ik})^m (d_{ik})^2 \quad (1)$$

$$u_{ik} = \frac{1}{\sum_{j=1}^{c}\left(\frac{d_{ik}}{d_{jk}}\right)^{2/(m-1)}} \quad (2)$$

d_{ik}^2 is the distance between the k th data (pixel value) and the center of the i th cluster and v_i denotes the center value of the i th cluster, which are defined by equations (3) and (4) as follows:

$$d_{ik}^2 = \| x_k - v_i \| \quad (3)$$

$$v_i = \frac{\sum_{k=1}^{n}(u_{ik})^m x_k}{\sum_{k-1}^{n}(u_{ik})^m} \quad (4)$$

where x_k is the intensity of the k th pixel, n is the number of data (pixels), c is the number of clusters, and m is the exponent weight.

The pixels of the input image are divided into three clusters. The first cluster includes pixels in the background (low intensity). The second cluster includes pixels in the tumor region (medium intensity) and the third cluster includes pixels in the liver region other than tumor (high intensity). The tumor region is outputted for further analysis.

C. Wavelet based Texture Feature Extraction

Texture is one of the most used characteristics in medical image interpretation, and is applicable to a wide variety of image processing problems. For example, it is difficult to classify human body organ tissues using shape or gray level information because the shape of each organ is not consistent throughout all 2D slices of a medical image and the gray level intensities overlap considerably for soft tissues. However, tissues are expected to have consistent and homogeneous textures along with the series of slices. Therefore, texture information can be used to discriminate among different organ tissues [10].

A major class of feature extractors relies on the assumption that texture can be defined by the local statistical properties of pixel gray levels. From the image histogram, first order statistics can be derived and used as texture features. It was soon argued that they did not suffice for adequate texture description and that second order statistics were required, as efficiently reflected in features computed from the co-occurrence matrix [15]. The conjecture that second order statistics suffice for texture analysis were later rejected [16] and various other texture analysis scheme were introduced [3]. The most commonly used texture features that have been applied successfully to real world textures are the SGLDM [15], the Fourier Power Spectrum (FPS) [17], the Gray Level Difference Statistics (GLD) [18] and the Law's Texture Energy Measures (TEM) [19].

A weakness shared by these entire texture analysis schemes is that the image is analyzed at one single scale, a limitation that can be avoided by employing multiscale representations [20]. Studies in the human visual system support this approach since researchers have found that the visual cortex can be modeled as a set of independent channels, each with a particular orientation and spatial frequency tuning. Several multichannel texture analysis schemes have been developed. In the last decade, wavelet theory has emerged and became a mathematical framework which provides a more formal, solid and unified framework for multiscale analysis [21]. The 2D Discrete Wavelet

Transform (DWT) is computed by applying a separable filter bank to the image.

$$L_n (bi,bj) = [H_x * [H_y * L_{n-1}] |2,1]_{|1,2} (bi,bj) \quad (5)$$

$$D_{n1} (bi,bj) = [H_x * [G_y * L_{n-1}] |2,1]_{|1,2} (bi,bj) \quad (6)$$

$$D_{n2} (bi,bj) = [G_x * [H_y * L_{n-1}] |2,1]_{|1,2} (bi,bj) \quad (7)$$

$$D_{n3} (bi,bj) = [G_x * [G_y * L_{n-1}] |2,1]_{|1,2} (bi,bj) \quad (8)$$

[* denotes the convolution operator, $|2,1|_{|1,2}$ sub sampling along the rows (columns) and $L_0 = I$ is the original image]. H and G are a low and bandpass filter respectively. L_n is obtained by lowpass filtering and is therefore referred to as the low resolution image at scale n. The detail images D_{ni} are obtained by bandpass filtering in a specific direction and contain directional detail information at scale n. The original image I is thus represented by a set of sub images at several scales:

$\{ L_d, D_{ni} \}_{i = 1,2,3, n = 1 \ldots d}$ which is a multiscale representation of depth d of the image I.

In this work, the biorthogonal wavelet transform is applied on the liver region to obtain Horizontal (D_{11}), Vertical (D_{12}) and Diagonal (D_{13}) details of images. A biorthogonal filter was utilized in the decompositions. The selection of biorthogonal over orthonormal was made because of smoothness and their robustness under slight shifts of image components. Since each wavelet coefficient $D_{ni}(bi,bj) \in R$ and the co occurrence matrix is defined for an image with a countable number of gray levels, the co occurrence matrix $C_{ni}^{d\theta}$ can be defined. The element (j, k) of the co occurrence matrix $C_{ni}^{d\theta}$ is defined as the joint probability that a wavelet coefficient $D_{ni} = j$ co occurs with a coefficient $D_{ni} = k$ on a distance d in direction θ. Usually, small values for d are used since most relevant correlation between pixels exists on small distance. From the three detail images three SGLDM or co occurrence matrixes $C_{11}^{d\theta}$, $C_{12}^{d\theta}$ and $C_{13}^{d\theta}$ are constructed. In this work 1 is used for d and 0, 45, 90 and 135 degrees are used for θ.

Gletsos, et al [9] used 8 optimum features extracted from the SGLDM statistical texture features and Mean in the gray level domain, for the classification of liver diseases. With this set Standard deviation (Std) which describes the contrast of the image are added to get 10 features for the feature set in this work. Hence, from each matrix, the 10 features namely Mean, Std, ASM, Contrast, Entropy, Homogeneity, Correlation, Sum of squares, IDM and Cluster tendency and hence totally 30 features are extracted.

D. Feature Selection

Feature selection is the process of choosing a subset of features relevant to a particular application. Optimized feature selection reduces data dimensionality and potentially removes noise, thus resulting in CAD tools that are not only more accurate but also more robust. Several CAD applications have demonstrated the positive impact of optimized feature selection.

Feature selection algorithms are categorized into exponential, randomized and sequential algorithms. Exponential algorithms (e.g. branch and bound, exhaustive) have exponential complexity in the number of features and are expensive to use (i.e. they have complexity $O(2^d)$ where d is the number of features). Randomized algorithms include genetic and simulated annealing search methods. They give optimum solution in very large search space. Sequential search algorithms have polynomial complexity (i.e. $O(d^2)$). They add or subtract features and use a hill climbing strategy.

Sequential forward selection (SFS) begins with zero attributes, evaluates all feature subsets with exactly one feature, and selects the one with the best performance. It then adds to this subset the feature that yields the best performance for subsets of the next larger size. This cycle repeats until no improvement is obtained from extending the current subset. Sequential backward selection (SBS) begins with all features and repeatedly removes a feature whose removal yields the maximal performance improvement.

In this work, SBS was made to select the optimal feature set because search space is minimum based on the classification performance of the feature subsets using PNN classifier.

E. Probabilistic Neural Network Classifier

Neural networks are ideal in recognizing a disease using representative examples since there is no need to provide a specific algorithm on how to identify the disease [22],[23]. The PNN provides a general solution to pattern classification problem by following the probabilistic approach based on the Bayes formula [24],[25].

III. PERFORMANCE EVALUATION

The performance of the system is evaluated with the radiologist and the patient's doctor. The performance of the PNN is compared with the performance of the Learning Vector Quantization (LVQ) Neural Network [26] to prove the choice of the classifier. Also, the performance of the system is compared with the performance of the PNN in the gray level domain for the selected feature set to prove the choice of wavelet domain.

IV. IMPLEMENTATION AND RESULTS

Images acquired were in DICOM (Digital Imaging and Communications in Medicine) format. They were collected from 20 hepatocellular carcinoma patients(HCC), 20 cholangio carcinoma patients (CC), 20 hemangioma(H) patients and 10 hepato adenoma(HA) patients. From these patients, 60 hepatocellular carcinoma slices (images), 60 cholangiocarcinoma slices (images), 60 hemangioma slices (images) and 30 hepato adenoma slices (images) are considered for this work. The system was implemented using the functions available in MATLAB.

Fig. 2a is a CT scan image of a patient with a liver tumor. The liver is located along the left half of the image and is light gray in color. The white tubular structures are the normal liver blood vessels. The liver tumor is dark and located on the edge of the liver and extends toward a blood vessel. The window with the liver and other fragments of organs are selected by removing 30 rows and 50 columns since this area usually does

not contain liver in the slices (Fig. 2b). Histogram for the window slice, Histogram after adaptive threshold decision, Liver region after the morphological operations and Segmented Tumor region after Fuzzy C Means Clustering Technique are given in Fig. 2c – Fig. 2f.

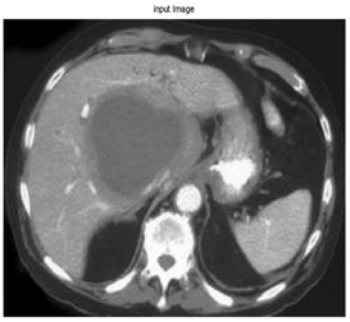

Fig. 2a CT abdominal image

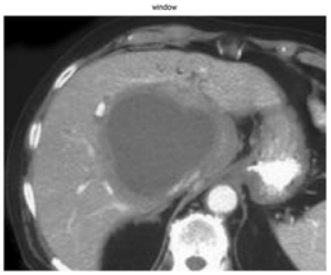

Fig. 2b Window slice

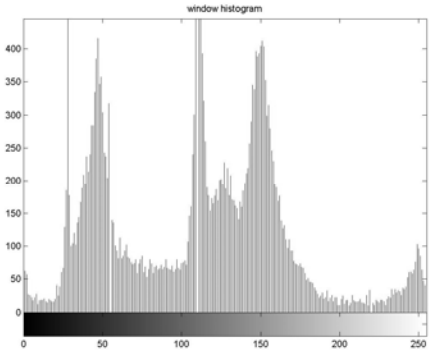

Fig. 2c Histogram of the window slice

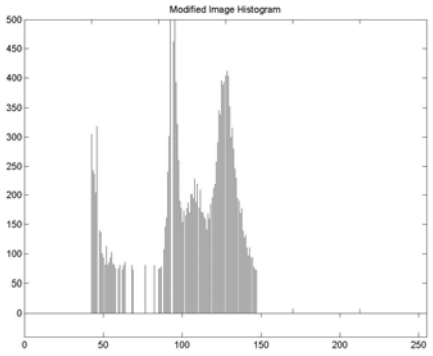

Fig. 2d Histogram after adaptive Threshold decision

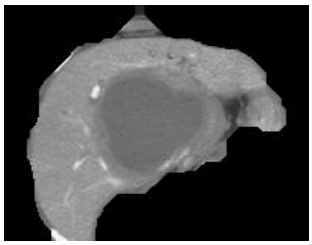

Fig. 2e Segmented Liver

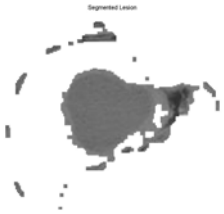

Fig. 2f Segmented Tumor

Segmented tumor and the percentage of affected area in the liver for hemangioma and cholangiocarcinoma tumor are given in Table 1.

TABLE I
SEGMENTED TUMOR AND THE PERCENTAGE OF THE AFFECTED AREA

Liver Tumor	Liver Image	Tumor region	% of affected area
Hemangioma (H)	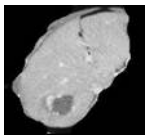		9.89
Cholangio Carcinoma (CC)			48.44

After extracting the tumor, the features were extracted as given in the feature extraction algorithm and the optimized feature set was selected by SBS based on the classification performance of PNN. From the experiments conducted for feature selection, it is found that the optimal feature set which gives good classification performance are Contrast, Entropy, Homogeneity, ASM of Horizontal, Vertical and Diagnonal details of image. Hence for this application domain, the above 12 features are enough for classifying the tumor as hepatocellular carcinoma, cholangio carcinoma, hemangioma and hepatoadenoma. These 12 features from a single image form a feature vector.

The input data set is divided into 2 different groups of training set and testing set to conduct the experiment. Data set size is tabulated in Table 2.

TABLE II
DATA SET USED TO CONDUCT EXPERIMENT

Disease Name	Patinet (nos)	Representative Slices (nos)	Training Set (nos)	Testing Set (nos)
HCC	20	60	30	30
CC	20	60	30	30
H	20	60	30	30
HA	10	30	15	15

The training set and testing set in each group are disjoint. To prove the validity of the testing, while testing, care must be taken so that the slices collected from a patient are not added in the training set. These 2 groups of dataset are used to train and test the LVQ and PNN. The experiment is repeated for 5 sets with different training and testing set. The set which gives a maximum classification performance is chosen for calculating the accuracy.

With the available data and the experiments conducted, it is found that the LVQ neural network with 0.01 as a learning rate for the 48 hidden neuron and 500 epochs produces an accuracy of 83.5%. The PNN network with the 12 input neurons in the input unit for giving the feature values, 105 neurons in the pattern unit for storing the weight value for each pattern and 4 neurons in the summation unit for the 4 classes produces an accuracy of 90.2%. Two different sets of training and testing set were used.

Performance of the system is evaluated for the 105 images. For the same feature set namely Contrast, Entropy, Homogeneity and ASM extracted from the image directly, without applying biorthognal transform, the performance of the classifier PNN and LVQ are also evaluated. Results are tabulated in Table 3 to Table 6.

TABLE III
CONFUSION MATRIX FOR THE TEXTURE FEATURES USING PNN IN WAVELET DOMAIN

Correct Class	Classified as			
	HCC	CC	HA	H
HCC	30	0	0	0
CC	1	28	0	1
HA	3	0	12	0
H	2	1	0	27

TABLE IV
CONFUSION MATRIX FOR THE TEXTURE FEATURES USING LVQ IN WAVELET DOMAIN

Correct Class	Classified as			
	HCC	CC	HA	H
HCC	28	2	0	0
CC	3	24	0	3
HA	3	0	10	2
H	2	2	0	26

TABLE V
CONFUSION MATRIX FOR THE TEXTURE FEATURES USING PNN IN GRAYLEVEL DOMAIN

Correct Class	Classified as			
	HCC	CC	HA	H
HCC	27	2	0	1
CC	2	26	0	2
HA	4	0	10	1
H	4	2	0	24

TABLE VI
CONFUSION MATRIX FOR THE TEXTURE FEATURES USING LVQ IN GRAYLEVEL DOMAIN

Correct Class	Classified as			
	HCC	CC	HA	H
HCC	26	2	0	2
CC	3	19	0	8
HA	4	0	10	1
H	4	2	0	24

From the above data, the accuracy i.e. the recognition rate of the classifiers is calculated as given in the equation (9) and the results are given in the Figure 3.

$$Accuracy = \frac{Total\_No\_of\_correctly\_classified\_images}{Total\_No\_of\_images} \quad (9)$$

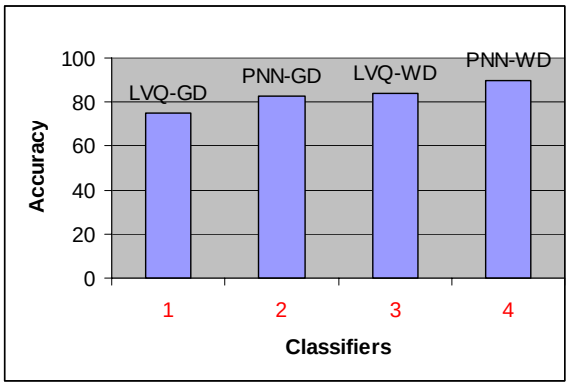

Fig. 3 Classification Performance

From the Fig. 3, it is clear that the selected features extracted from the wavelet domain by applying biorthogonal transform produces high classification accuracy (recognition rate) in the order of 90.2%. The classifiers LVQ and PNN show performance improvement for the selected features extracted after applying biorthogonal wavelet transform. In the wavelet domain also PNN outperforms LVQ with the difference of 6% in the recognition rate.

Results show that, the performance of the classifiers LVQ and PNN can be improved by combining the biorthogonal wavelet transform and the optimized second order statistical features. Both are good classifiers. But based on the accuracy and the training speed, since PNN outperforms LVQ, the proposed methodology uses PNN as a classifier for classifying tumor.

Accuracy depends on the class distribution in the training data set. Hepato adenoma tumor is not classified correctly because of the inadequate samples. A good distribution of samples is needed to construct the useful model.

Generally speaking, the initialization of the classifier, training samples, learning rate, number of epochs and the number of hidden neurons affect the diagnostic result of the system. Use of large databases of CT images collected from patients, is expected to improve the system robustness and ensure the repeatability of the resulted performance. But for PNN, since the number of neurons in the pattern unit depends on the number of training samples, memory requirement is more. Since memory cost is low, this is not a significant drawback. Speed is high compared with LVQ.

With the available data and the experiments conducted, it is found that the second order statistical features derived from wavelet coefficients can be used as a texture feature for classifying tumors. Results are also evaluated with radiologists. The patients' disease nature was confirmed by the medical specialists after taking biopsy. This is taken as a gold standard for comparing the classification results.

The benign tumors like focal nodular hyperplasia which are not commonly encountered are not considered in this study. Hence the system may give a wrong result if this tumor is given for testing. But the PNN can easily be retrained, for the incoming new samples. Hence the proposed system is an adaptable system. Learning procedure is also not time consuming. Since the proposed system follows the component based model, each module can be replaced by a best one in the future.

V. Conclusion

The proposed system is used to segment the tumor with considerable satisfaction. Results are evaluated with radiologists. Biorthogonal wavelet based texture features can be extracted and used to train the PNN to classify the liver tumor as hepatocellular carcinoma, cholangio carcinoma, hepatocellular adenoma and hemangioma with better performance to help radiologists and medical specialists during their medical decision process. The proposed system can be extended for other types of images or for other classes of liver diseases, provided that the feature vectors are reevaluated and the neural networks are retrained. The findings of this work may also suggest a much easier hardware implementation of tissue analysis functions to be provided in image acquisition machines like CT scanners in the future. This can be helpful for teaching and for fresher to improve their diagnostic accuracy.

References

[1] Heiken J.P, Wegman P.J and Lee J.K.T, "Detection of focal hepatic masses: Prospective evaluation with CT, delayed CT, CT during arterial portography and MR imaging", Radiology, vol. 171, pp. 47-51, 1989.

[2] E-Liang Chen, Pau-CHoo Chung, Ching-Liang Chen, Hong-Ming Tsai and Chein I Chang, "An Automatic Diagnostic system for CT Liver Image Classification", IEEE Transactions Biomedical Engineering, vol 45, no. 6, pp. 783-794, June 1998.

[3] Chung-Ming Wu, Yung-Chang Chen, Kai-Sheng Hsieh, "Texture features for Classification of Ultrasound Liver Images", IEEE Transactions on Medical Imaging, vol 11, no 2, pp. 141-152, June 1992.

[4] Yasser M. Kadah, Aly A. Farag, Jacek M. Zaruda, Ahmed M. Badawi, and Abou-Bakr M. Youssef., "Classification Algorithms for Quantitative Tissue Characterization of Diffuse Liver Disease from Ultrasound Images," IEEE transactions on Medical Imaging Vol 15, No 4, pp 466-477, August 1996.

[5] Aleksandra Mojsilovic, Miodrag Popovic, Srdjan Markovic and Miodrag Krstic, "Characterization of Visually Similar Diffuse Diseases from B-Scan Liver Images using Non Separable Wavelet Transform", IEEE Transactions on Medical Imaging, vol. 17, no. 4, pp. 541-549, Aug. 1998.

[6] E-Liang Chen, Pau-CHoo Chung, Ching-Liang Chen, Hong-Ming Tsai and Chein I Chang, "An Automatic Diagnostic system for CT Liver Image Classification", IEEE Transactions Biomedical Engineering, vol 45, no. 6, pp. 783-794, June 1998.

[7] Pavlopoulos.S, Kyriacou.E, Koutsouris.D, Blekas.K, Stafylopatis.A, Zoumpoulis.P, "Fuzzy Neural Network-Based Texture Analysis of Ultrasonic Images," IEEE Engineering in Medicine and Biology, pp 39-47, Feb 2000.

[8] Jae-Sung Hong, Toyohisa Kaneko, Ryuzo Sekiguchi and Kil-Houmpark, "Automatic Liver Tumor Detection from CT", IEICE Trans. Inf.& Syst.,Vol. E84-D, No. 6, pp 741-748, June 2001.

[9] Gletsos Miltiades, Stavroula G Mougiakakou, George K. Matsopoulos, Konstantina S Nikita, Alexandra S Nikita, Dimitrios Kelekis, "A Computer-Aided Diagnostic System to Characterize CT Focal Liver Lesions: Design and Optimization of a Neural Network Classifier," IEEE Transactions on Information Technology in BioMedicine, Vol 7, Issue 3, pp 153 – 162, Sep. 2003.

[10] John.E.Koss, F.D.Newman FD, T.K.Johnson, and D.L.Kirch, "Abdominal Organ Segmentation Using Texture Transforms and a Hopfield Neural Network", IEEE Transactions on Medical Imaging, vol 18, no. 7, pp 640-648, July 1999.

[11] Chien Cheng Lee, Pau-Choo Chung, Hong-Ming Tsai, "Identifying Abdominal organs from CT image series using a Multimodule Contextual Neural network and Spatial Fuzzy rules", IEEE Transactions on Information Technology in Biomedicine, vol 7, no. 3, pp. 208-217, Sep. 2003.

[12] Lee.W.L, Chen.Y.C, and Hsei.K.S., "Ultrasonic liver tissues classification by fractal feature vector based on M-band wavelet transform," IEEE Trans. Med. Imaging, vol. 22, pp. 382–392, Mar. 2003.

[13] Yu-Len Huang, Jeon-Hor Chen1, Wu-Chung Shen1 "Computer-Aided Diagnosis of Liver Tumors in Non-enhanced CT Images" Department of Computer Science and Information Engineering, Tunghai University, Mid Taiwan, Journal of Medical Physics, Vol. 9, pp. 141-150, 2004.

[14] Robert M Haralick, Stanely R Sternberg and Xinhua Zhuang, "Image analysis using Mathematical Morphology", IEEE Transactions on Pattern Analysis and Machine Intelligence, vol. PAMI-9, no. 4, pp. 532-549, July, 1987.

[15] Robert.M, Haralick, K. Shanmugam, Dinstein, "Texture Features for Image Classification", IEEE Transactions on Systems, Man, and Cybernetics, Vol.SMC-3, No. 6, pp 610-621, Nov. 1973.

[16] A.Gagalowicz, "A new method for texture field synthesis: Some applications to the study of human vision", IEEE Transactions on Pattern Analysis and Machine Intelligence, vol. PAMI-3, pp. 520-533, 1982.

[17] G.O. Lendaris and G. L. Stanley, "Diffraction pattern sampling for automatic pattern recognition," Proceedings. IEEE, vol. 58, pp. 198-216, 1970.

[18] J.S. Weszka, C.R. Dryer, and A. Rosenfeld, "A comparative study of texture measures for terrain classification," IEEE Trans. Syst., Man,Cybern., vol. SMC-6, pp. 269-285, 1976

[19] K. I. Laws, "Texture energy measures," Proc. Image Understanding Workshop, pp. 47-51, 1979.

[20] Van.G. Wouwer, P. Scheunders, and D. Van Dyck, "Statistical texture characterization from discrete wavelet representations," IEEE Trans.Image Processing, vol. 8, pp. 592–598, Apr. 1999.

[21] Mallat.S.G.,"A theory for multiresolution signal decomposition: A wavelet representation", IEEE Transactions on Pattern Analysis and Machine Intelligence. Vol. 11, pp 674-693, July 1989.

[22] P. P. Raghu and B. Yegnanarayana, "Supervised Texture Classification Using a Probabilistic Neural Network and Constraint Satisfaction Model, IEEE Transactions on Neural Networks, vol. 9, no. 3,pp 516-522, May 1998

[23] Sujana.H, S. Swarnamani, and S. Suresh, "Artificial neural networks for the classification of liver lesions by image texture parameters," Ultrasound Med. Biol., vol. 22, pp. 1177–1181, Sept. 1996.

[24] Donald.F.Specht, "Probabilistic neural networks", Neural Networks, vol. 3, pp. 109-118, 1990.

[25] Donald.F.Specht, "Probabilistic neural networks and the Polynomial Adaline as complementary techniques for pattern classification", IEEE Transactions on Neural Networks, vol 1, no 1, pp 111 – 121, March 1990.

[26] www.dacs.dtic.mil/techs/neural/neural7.html

K.Mala did her B.E.(Hons.) in Computer Science and Engineering in 1989 in Thiagarajar College of Engineering, Madurai, Tamilnadu, India. Completed her M.S.(Software Systems) in BITS, Pilani in 1998. Currently pursuing Ph.D. under the guidance of Dr.V.Sadasivam in Manonmaniam Sundaranar University, Tirunelveli, Tamilnadu, India. Also working as a Senior Lecturer in Mepco Schlenk Engineering college, Sivakasi, Tamilnadu, India. Area of interest are Medical image processing and Neural Networks. Life member in ISTE and student member in IEEE.

Dr.V.Sadasivam did his B.E. in Electrical and Electronics Engineering in 1973 in Thiagarajar College of Engineering, Madurai, Tamilnadu, India. He completed his M.Sc.(Power Systems) in 1975 from Coimbatore Institute of Technology, Coimbatore, Tamilnadu, India. He obtained his Ph.D. in 1993 from Anna University in 1993. Currently he is working as Professor and Head in Computer Science and Engineering Department in Manonmaniam Sundaranar University, Tirunelveli, Tamilnadu, India.

Dr.S.Alagappan, M.D. is currently working as a Chief Radiologist in Devaki MRI & CT Scans, Madurai, Tamilnadu, India. He got more than 20 years of experience in medical field.